General Disclaimer

One or more of the Following Statements may affect this Document

- This document has been reproduced from the best copy furnished by the organizational source. It is being released in the interest of making available as much information as possible.

- This document may contain data, which exceeds the sheet parameters. It was furnished in this condition by the organizational source and is the best copy available.

- This document may contain tone-on-tone or color graphs, charts and/or pictures, which have been reproduced in black and white.

- This document is paginated as submitted by the original source.

- Portions of this document are not fully legible due to the historical nature of some of the material. However, it is the best reproduction available from the original submission.

Produced by the NASA Center for Aerospace Information (CASI)

TECHNICAL REPORT NO. 1

REDUCTION OF THE ONE-DIMENSIONAL X-RAY SCATTERING DATA ON
MIRROR FLATS AT NASA/MSFC

Prepared for

NASA/MSFC
George C. Marshall Space Flight Center
Huntsville, AL   35812

Contract NAS8-34591

By

Alton C. Williams
Alabama A. & M. University
Normal, AL   35762

MAY 1983
RECEIVED
NASA STI FACILITY
ACCESS DEPT.
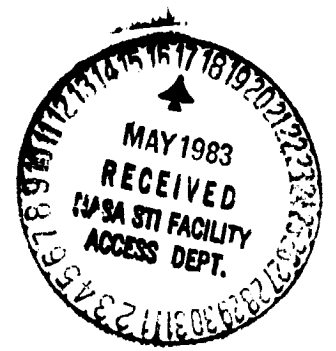
NOVEMBER 1981

REDUCTION OF THE ONE-DIMENSIONAL X-RAY
SCATTERING DATA ON MIRROR FLATS AT NASA/MSFC

I. General Discussion of Measurements

The X-ray scattering facility at NASA/MSFC has been utilized to obtain data on the scattering of X-rays from various mirror flats obtained from different vendors. The scattering data discussed in this section is that obtained by a one dimensional proportional counter at x-ray energies of 8.06, 6.4 and 2.99 keV.

The basic experimental set up is as follows. X-rays are generated at one end of a 312.4 meter long tube which is under vacuum. This long tube provides a parallel beam of x-rays which is then collimated by a slit and allowed to scatter from a pair of mirror flats at small grazing angles of incidence. The pair of mirror flats are in periscope geometry so that the scattered beam is parallel to the incident beam. The slit and mirrors assembly is placed 182.4 meters from the other end of the tube where the proportional counter detector is located.

The detector, itself, is sitting on an optical table which is pivoted so that the detector can rotate to intercept x-rays at a range of spatial locations. The optical table pivot is located 2.78 meters in front of the detector (towards the incoming x-rays), and it has an operational angular range of 350 arc minutes which corresponds to an arc length of 0.283 meters (11.13 in). Measured from the position of the mirror, this total angular range of the data is (350) (2.78/182.4)

= 5.33 arcminutes.

Because angles can be measured both with respect to the optical table pivot as well as with respect to the position of the mirrors assembly, it is necessary to distinguish between these two. The angles measured with respect to the optical table pivot will be designated by "Table angles"; whereas, angles measured with respect to the mirrors will be designated by the angles without the "table" prefix. Hence, the range of data that is taken with the one dimensional proportional counter is 350 table arc minutes or 5.33 arcminutes. To convert from one to the other, one can use the relation

$$\theta = \frac{L_1}{L_2} \theta_T = .0151 \; \theta_T$$

Where L_1 = distance from the optical table pivot to the detector and L_2 = distance from the mirrors assembly to the detector. θ_T is the table angle and θ is the angle measured with respect to the mirrors assembly.

In the gathering of data, the following is done. Electronically, the linear anode wire of the detector is divided into 1,024 equal segments. X-rays incident within a given segment will then be accumulated in the corresponding channel of a 1,024 channel multi-channel analyzer. With the optical table at a given position, data is taken at the grazing angles of incidence of 0' (direct slit), 25', 39', and 51'. The table is then rotated to get another (but overlapping) field of view. Also, data is taken at two different table positions on the direct slit image

so that a correlation between number of channels and table angles can be made. Background runs (without x-rays on) are made each day data is taken.

Some special measurements have been made to calibrate the response of the detector as a function of position on the anode wire. Basically, the 1,024 different segments of the wire do not all respond to incident x-rays equally efficiently. The measurements consist of removing the mirrors and slit assembly and illuminating the entire anode wire. For a uniform flux of x-rays, any deviations in a constant number of counts in all of the 1,024 channels indicate a variation in the efficiency of parts of the wire. This data was taken at two different table positions so that effects due to a non-uniform beam could be removed. This was done for all x-ray energies of interest.

II. Description of Typical Result

All the data taken for a given mirror at a particular grazing angle of incidence and x-ray energy was combined to give a single spectrum corrected for background and for deviations in the relative efficiencies of different portions of the anode wire of the proportional counter.

Measuring from the peak of each image, a typical spectrum covers the angular range of from -50 arcseconds to 280 arcseconds. Since there is data on both sides of the peak, a measure of the asymmetry of the image can be given. Typically, the asymmetry is below 20%. There

were some highly asymmetric images which apparently indicates that something is wrong with the data such as poor zero angle alignment.

Data which extends further on one side of the peak is used for the other side assuming that the image should be symmetric. This then gives a spectrum which covers the angular range, typically, of ±280 arcseconds measured from the peak. A summary package of each spectrum is given by the computer software which includes the following:

1. A printout of total counts, angular range of the data taken, the full-width-half-maximum, the percent asymmetry, the reflectivity and a table showing the integrated fraction of counts in the image as a function of the angle ±θ measured from the peak. This fraction of counts is given for both the image itself and relative to the direct slit image.

2. A plot showing the entire image is made. See figure 1 for a typical result. This plot is made on microfiche for convenience in filing. A hard copy can be obtained when desired.

3. A second plot is made which shows a blow-up of the image around the peak. This allows one to see the structure in the image better. Figure 2 shows a typical plot of this kind.

4. A third plot is made which shows the integrated fraction of counts as a function of the angle, ±θ, measured from the peak. This curve always goes to the value of 1.0 at the maximum angle at which data was taken. The slope of this curve at the maximum angle gives an indication as to whether

there is more counts in the image outside the maximum
angle. Zero slope would indicate no more counts. A typical
plot of this kind is shown in figure 3. As is true for this
sample plot, it is generally true that the curve rises very
rapidly reaching a plateau close to its maximum value of
1.0 within a few table arcminutes. This apparently indicates
that most of the flux is within the central core of the image
with very little scattered flux.

5. A fourth plot is made which blows up the integrated fraction
    curve out to about 5 table arcminutes. This allows one to
    look at the details in the rapidly rising part of this curve.
    A more slowly rising curve than that for the direct slit
    image indicates a spreading out of the peak due to a com-
    bination of figure distortion and scattering due to the
    roughness of the mirror surfaces. A typical plot of this
    kind is shown in figure 4.

The angular resolution of the data is determined by the facts that
-1 channel of the multichannel analyzer covers an angular range of about
8.3 table arcseconds and that the inherent resolution of the detector
is about 0.5 mm which corresponds to about 37 table arcseconds. In
terms of the angle measured from the mirror assembly, this 37 table
arcseconds corresponds to 0.56 arcseconds.

Calculation of the statistical error in the data is shown in Appendix A. As a typical example of the error in the data, the data on the PE-II-003 (ULE/Ni) mirror at the x-ray energy of 2.99 keV is given below.

Grazing Angle of Incidence	Total Counts	FWHM	Reflectivity
0' (Dir. Slit)	7399 ± 86	0.75 ± .13	--
25'	6295 ± 79	2.01 ± .17	0.92 ± .01
39'	4767 ± 69	2.27 ± .19	.80 ± .01
51'	1946 ± 54	0.75 ± .13	.63 ± .01

III. Collected Results To Data

All data collected with the one dimensional detector between the period November 5, 1980 and May 14, 1981 has been analyzed. This includes the following thirteen mirrors:

Vendor	Substrate	Coating	X-ray Energist (keV)
Eastman-Kodak	Zerodur	Ni	2.99
Max Planck	Zerodur	Ni	2.99
Eastman-Kodak	Fused Silica	Pt	2.99, 6.4
Eastman-Kodak	Zerodur	Pt	2.99, 6.4
Perkin-Elmer	Zerodur	Au	2.99, 6.4, 8.06
Max Planck	Zerodur	Au	2.99, 6.4, 8.06
Perkin-Elmer	Ule	Ni	2.99, 6.4, 8.06
Eastman-Kodak	Ule	Ni	2.99, 6.4, 8.06
Perkin-Elmer (IR & D)	Ni-Be	Pt	2.99, 6.4, 8.06
Eastman-Kodak	Ule	Au (Recoated)	2.99, 6.4, 8.06
Eastman-Kodak	Fused Silica	Au	2.99, 6.4, 8.06
Perkin-Elmer	Zerodur	Pt	2.99, 8.06
Perkin-Elmer	Ule	Pt	2.99, 6.4, 8.06

The plots mentioned in section II for each scattering spectrum on these mirrors aregiven in appendix B. In appendix C is given a summary of the data for each angle, energy, and mirror. The items in the summary includes 1) the full-width half maximum, 2) the angle at which 50% of the counts fall within, 3) the fraction of the counts outside 14 arcseconds, 4) the measured reflectivity, 5) the theoretical reflection, and 6) a general comment on the data. When the general comment mentions "scuzz" it is referring to the fact that this data had a spurious source of counts in a certain spatial location which had nothing to do with x-rays from the mirrors or normal background. Hence, the fraction of counts within a given angle would not be meaningful for these spectra.

IV. Summary & Limitations

In general, the mirror surfaces are so smooth that there is very little scattering due to roughness. In retrospect, there are several things that should be done differently to obtain better data. Among these are the zero angle verification procedure, the mirror holder system, the calibration of the detector efficiency, and the optimization of the elevation of the detector. For these reasons, the data presented in this report should be taken as very qualitative. In particular, the measured reflectivities do not, in general, agree with the theoretical values because of one or nore of the problems mentioned above. Other information such as the FWHM and the fraction of counts outside 14 arcseconds is more reliable, however.

GENERAL FORMALISM FOR STATISTICAL ERRORS

I. Error in the Number of Counts

The usual assumption of using the square root of the number of counts as the uncertainty, σ, in these counts will be used:

$$\sigma_i = \sqrt{N_i} \qquad (A1)$$

where, N_i is either the number of counts in channel i, or the total number of counts in all channels of a given run i .

II. Error in Corrected Counts for Each Channel

Since the counts in each channel are corrected for background counts, as well as, for variations in the response of the detector as a function of the channel number, the error, σ_i', may be above and beyond that calculated by equation (A1). This will be examined now.

The corrected number of counts N_i' is calculated from the uncorrected number of counts N_i in each channel i by the relation:

$$N_i' = (N_i - N_B) \, RCE_i . \qquad (A2)$$

N_B is the number of background counts in each channel which is assumed to be a constant. RCE_i is the correction factor which corrects for the efficiency of channel number i . The equation for RCE_i is given in a separate article. The important equation for error analysis, however, is the following:

$$\sigma^2_{RCE_i} = (RCE_i)^2 \sum_{v=1}^{M_i} \left[\left(\frac{1}{N_{ij}(1)} + \frac{1}{N_{ij}(2)} \right) \right] + \frac{1}{N_i(1)} + \frac{1}{N_{i_0}(1)}$$

$$(A3)$$

Where $N_{ij}(1)$ and $N_{ij}(2)$ are in reference to the fact that to calculate RCE_i a data run had to be done with the detector located in two different spatial positions. $N_{ij}(1)$ is the number of counts in channel number ij when the detector is at location number 1, and $ij = i + j \cdot k$ where k is the number of channels between location 1 and location 2. i_0 is an arbitrary reference channel number normally taken as channel number 512. The summation contains M_i terms where

$$M_i = \frac{\lfloor i - 512 \rfloor}{k} \tag{A4}$$

As long as the channel numbers i are limited to channels which have reasonably good efficiencies, it is true that

$$N_{ij}(1) \approx N_{ij}(2) \approx N_i(1) \approx N_{i_0} \approx N_R . \tag{A5}$$

That is in the data taken to calibrate the efficiency of the detector, the number of counts in each channel are approximately equal to some average number N_R . For the data analyzed in this report:

$$N_R = \begin{cases} 500 & \text{Fe Line (1.94 \AA)} \\ 450 & \text{Ag Line (4.16 \AA)} \\ 700 & \text{Cu Line (1.54 \AA)} \end{cases} \tag{A6}$$

Hence, the variance in RCE_i can be written as

$$\sigma^2_{RCE_i} \approx \frac{(RCE_i)^2 \; (2 M_i + 2)}{N_R} \tag{A7}$$

In the counter efficiency runs used to calibrate the counter reponse efficiencies, the value of k in equation (A4) was about 244. Hence,

$$M_i = \frac{| i - 512 |}{244} \tag{A8}$$

Substituting for $\sigma_{RCE_i}^2$ from eq. (A7) this becomes

$$\sigma_{N_i'}^2 = (RCE_i)^2 \left[\sigma_i^2 + \frac{3N_i^2 (M_i + 1)}{N_R} \right] \quad (A16)$$

For the data analyzed in this report, the worst case is in the peak channel where typically these are 2300 counts. If it is also assumed that RCE_i and M_i are the worst case, then $RCE_i = 2$, $M_i = 2$, $N_{i2} = 450$ which gives $\sigma_{N_i}' = 535$ or a 23% error.

In channels which are not close to the peak, the second term in equation (A16) becomes negligible and the error reduces to the square root of the number of corrected counts.

III. Error in Total Counts for Corrected Data

The variance in the total number of counts for the corrected data is given by

$$\sigma_N^2 = \sum_i \sigma_{N_i'}^2 \quad (A17)$$

Since the dominant channel variance comes from the peak channel, this becomes

$$\sigma_N \approx \sigma_{pk} . \quad (A18)$$

As a typical example, consider the data taken on the PE-II-003 (ULE/Ni) mirror with Ag line x-rays. Near the peak $RCE \approx 1.33$. The total number of counts in the direct slit image is 7400; at 25' there are 6300 counts; at 39' there are 4800 counts; and at 51' there are 3000 counts. This gives the following errors:

Angle of Incidence	Total Counts	Error
0' (D.S.)	7400	± 194 (± 2.6%)
25'	6300	± 145 (± 2.3%)
39'	4800	± 115 (± 2.4%)
51'	3000	± 80 (± 2.7%)

IV. Error in Reflectivities

The "reflectivities" as quoted in this report are calculated with the equation.

$$R = \left[\frac{N_{Total} \ (Refl)}{N_{Total} \ (D.S.)} \right]^{\frac{1}{2}} \equiv \left(\frac{N_{TR}}{N_{TS}} \right)^{\frac{1}{2}} \tag{A19}$$

The variance in R is given by

$$\sigma_R^2 = \left(\frac{\partial R}{\partial N_{TR}} \right)^2 \sigma_{N_{TR}}^2 + \left(\frac{\partial R}{\partial N_{TS}} \right)^2 \sigma_{N_{TS}}^2$$

$$= \frac{R^2}{4 \ N_{TR}^2} \sigma_{N_{TR}}^2 + \frac{1}{4} \left(\frac{R^2}{N_{TS}^2} \right) \sigma_{N_{TS}}^2 \ . \tag{A20}$$

$$= \frac{R^2}{4} \left[\frac{\sigma_{N_{TR}}^2}{N_{TR}^2} + \frac{\sigma_{N_{TS}}^2}{N_{TS}^2} \right]$$

For the typucal mirror PE-II-003 (ULE/Ni) at the Ag line, the reflectivities and errors are given below:

Angle of Incidence	Reflectivity	Error
25'	0.92	$\pm$ .02
39'	0.80	$\pm$ .014
51'	0.63	$\pm$ .01

V. Error in the FWHM

Let M be the number of channels one has to go from the peak of the image before the number counts falls below one half of the peak value, and let $\bar{D}$ be the number of channels/table arc second ($\sim$ .12). Then,

$$\text{FWHM} = \frac{2M}{\bar{D}} \tag{A21}$$

This gives

$$\sigma_{\text{FWHM}} = \frac{\text{FWHM}}{\bar{D}} \ \sigma_{\bar{D}} \tag{A22}$$

The uncertainty in $\bar{D}$ is estimated from the data to be $\sigma_{\bar{D}} \approx .01$ with $\bar{D} = 0.12$. Hence,

$$\sigma_{\text{FWHM}} \approx (.083) \ \text{FWHM}. \tag{A23}$$

This number, known, may turn out to be less than the physical spatial resolution of the dector which is one channel or 8.3 table arcseconds (.125 arcseconds). Hence, σ_{FWHM} is given by

$$\sigma_{\text{FWHM}} = \text{Larger of} \begin{cases} (.083) \ \text{FWHM} \\ 0.13 \ \text{arcseconds} \end{cases} \tag{A24}$$

Figure 1.

MIRROR = P.E.-IR∿D(NI-BE/PT)

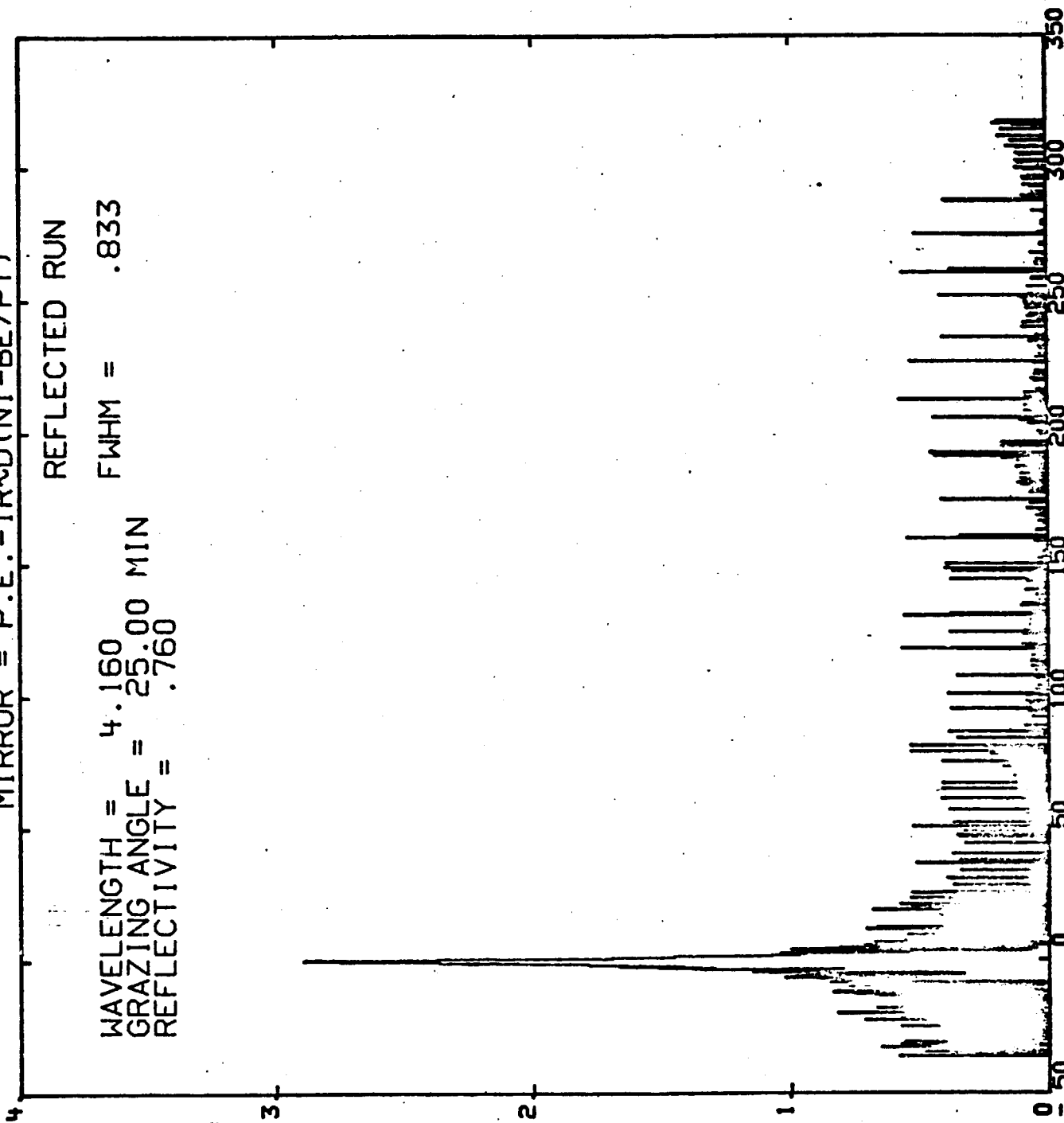REFLECTED RUN

WAVELENGTH = 4.160
GRAZING ANGLE = 25.00 MIN
REFLECTIVITY = .760

FWHM = .833

LOG COUNTS

TABLE ARCMINUTES

Figure 2.

MIRROR = P.E.-IR~D(NI-BE/PT)

REFLECTED RUN

FWHM = .833

WAVELENGTH = 4.160
GRAZING ANGLE = 25.00 MIN
REFLECTIVITY = .760

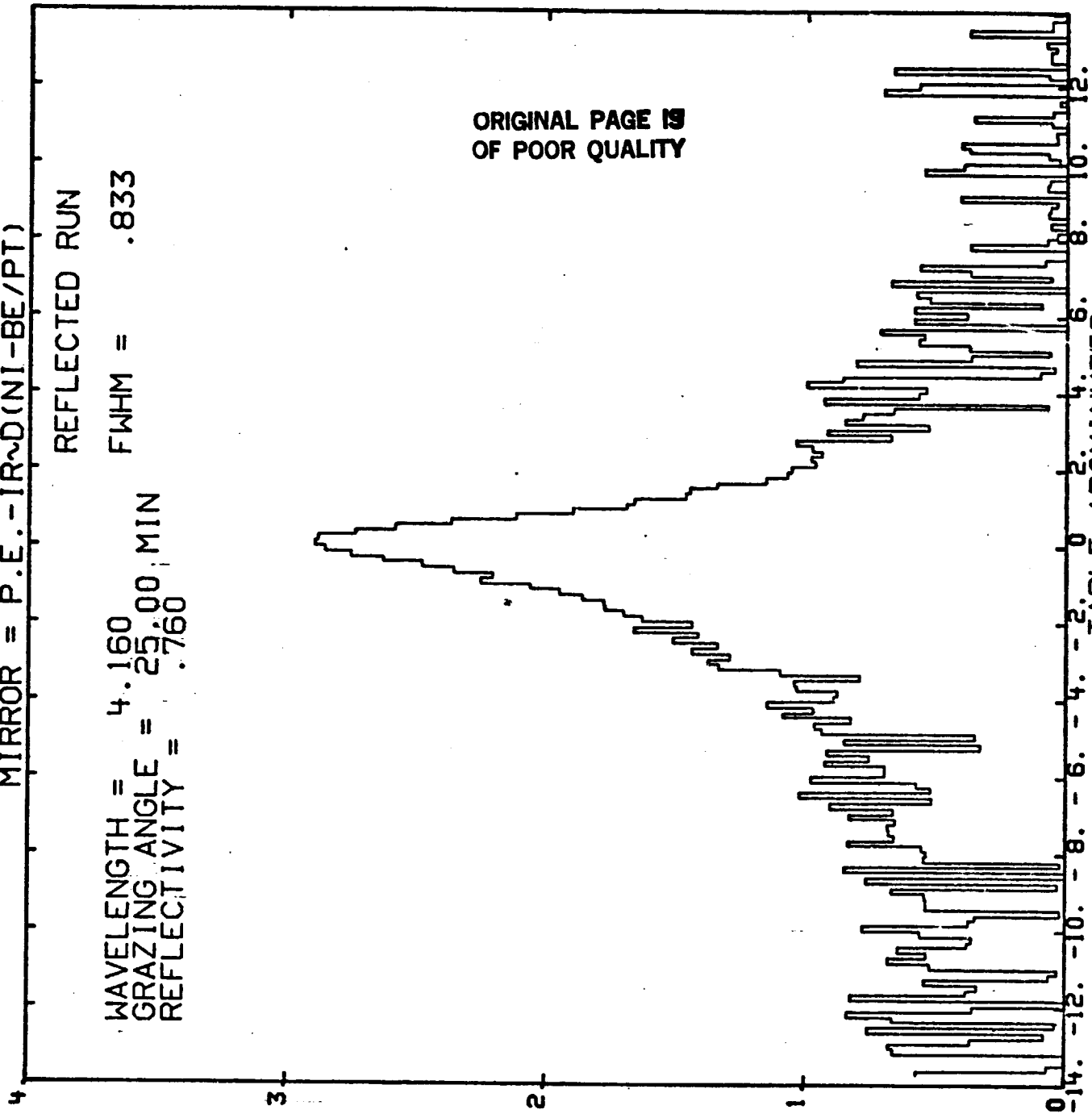ORIGINAL PAGE IS
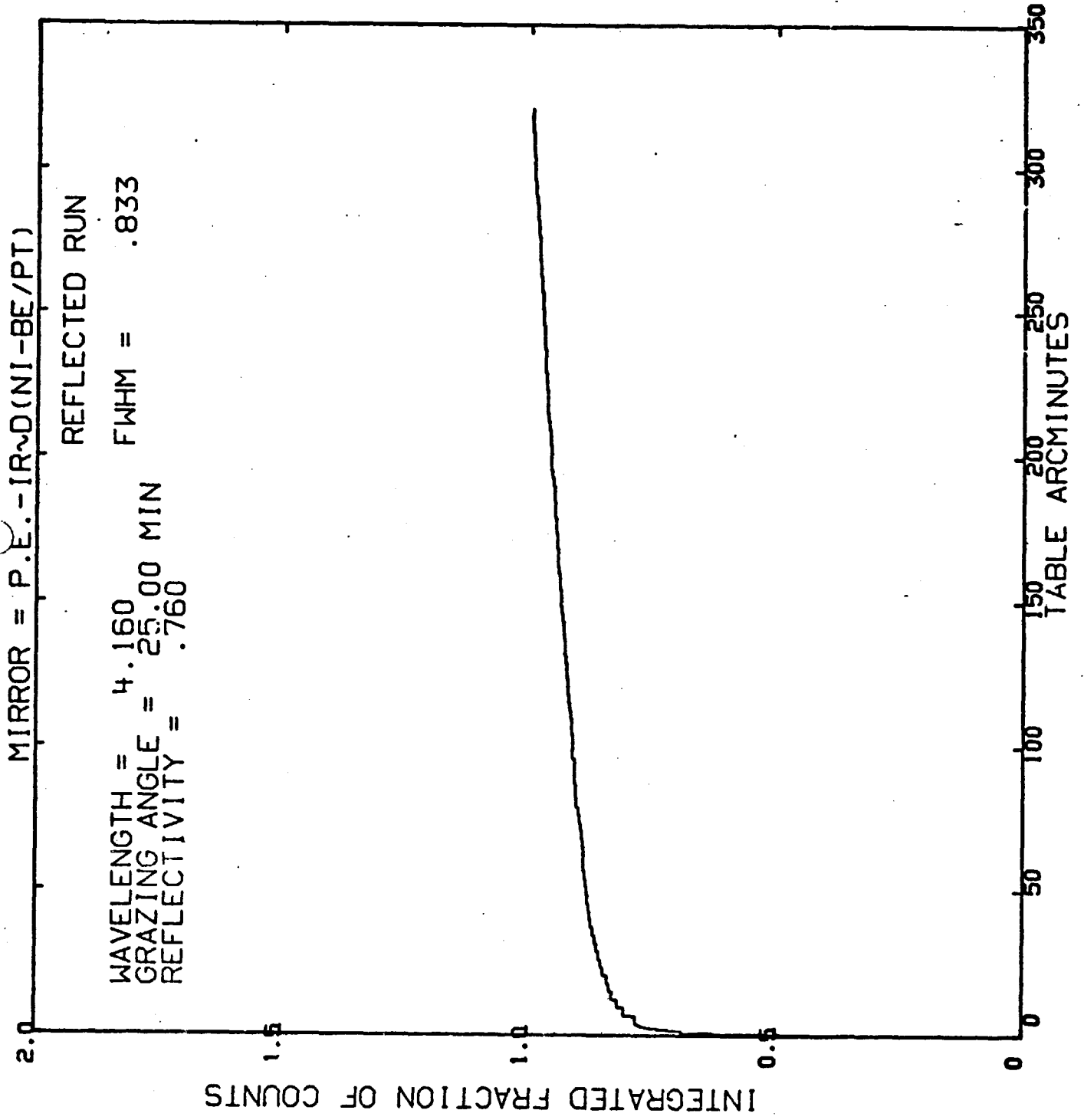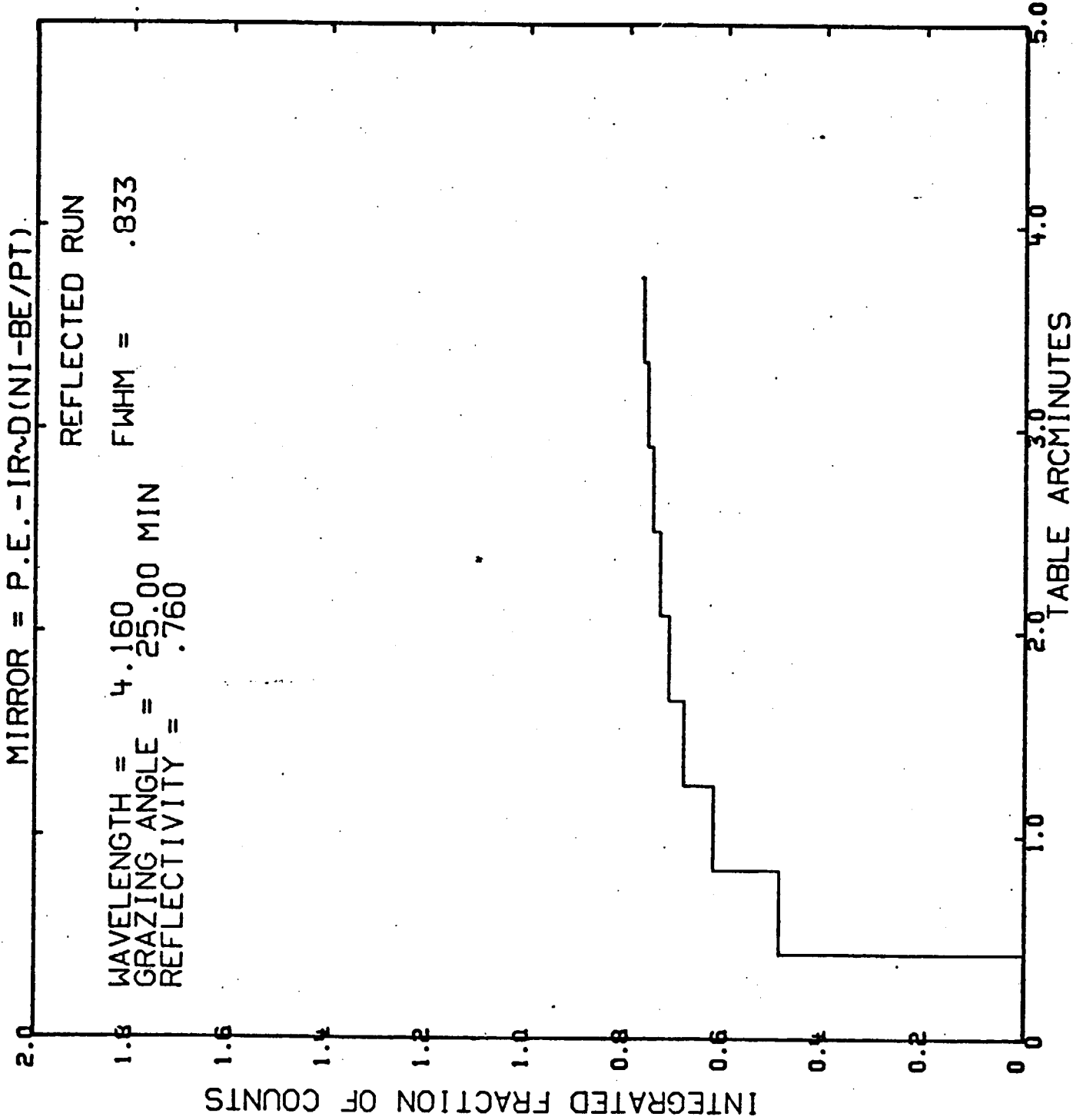OF POOR QUALITY

LOG COUNTS

TABLE ARCMINUTES

Figure 3.

MIRROR = P.E.-IR-D(NI-BE/PT)

REFLECTED RUN

FWHM = .833

WAVELENGTH = 4.160
GRAZING ANGLE = 25.00 MIN
REFLECTIVITY = .760

INTEGRATED FRACTION OF COUNTS

TABLE ARCMINUTES

Figure 4.

MIRROR = P.E.-IR~D(NI-BE/PT)

REFLECTED RUN

WAVELENGTH = 4.160   FWHM = .833
GRAZING ANGLE = 25.00 MIN
REFLECTIVITY = .760

INTEGRATED FRACTION OF COUNTS

TABLE ARCMINUTES